



Published in final edited form as:

Nature. 2014 December 4; 516(7529): 121–125. doi:10.1038/nature13980.

Piezo2 is the major transducer of mechanical forces for touch sensation in mice

Sanjeev S. Ranade¹, Seung-Hyun Woo¹, Adrienne E. Dubin¹, Rabih A. Moshourab^{2,+}, Christiane Wetzel², Matt Petrus³, Jayanti Mathur³, Valérie Bégay², Bertrand Coste^{1,†}, James Mainquist³, A.J. Wilson³, Allain G. Francisco¹, Kritika Reddy¹, Zhaozhu Qiu^{1,3}, John N. Wood⁴, Gary R. Lewin², and Ardem Patapoutian^{1,*}

¹Howard Hughes Medical Institute, Molecular and Cellular Neuroscience, Dorris Neuroscience Center, The Scripps Research Institute, La Jolla, California 92037, USA

²Department of Neuroscience, Max-Delbrück Center for Molecular Medicine, Robert-Rössle Straße 10, D-13092 Berlin, Germany.

³Genomics Institute of the Novartis Research Foundation, San Diego, CA 92121

⁴Molecular Nociception Group, Wolfson Institute for Biomedical Research, University College London, London WC1E 6BT, UK.

+Klinik für Anästhesiologie, m. S. operative Intensivmedizin, Campus Charité Mitte and *Virchow-Klinikum* Charité – Universitätsmedizin Berlin, Augustburgerplatz 1, 13353 Berlin

Summary

The sense of touch provides critical information about our physical environment by transforming mechanical energy into electrical signals¹. It is postulated that mechanically activated (MA) cation channels initiate touch sensation, but the identity of these molecules in mammals has been elusive². Piezo2 is a rapidly adapting (RA) MA ion channel expressed in a subset of sensory neurons of the dorsal root ganglion (DRG) and in cutaneous mechanoreceptors known as Merkel cell-neurite complexes^{3,4}. Merkel cells have been demonstrated to play a role in vertebrate mechanosensation using Piezo2, particularly in shaping the type of current sent by its innervating sensory neuron⁴⁻⁶. However, major aspects of touch sensation remain intact without Merkel cell activity^{4,7}. Here, we show that mice lacking Piezo2 in both adult sensory neurons and Merkel cells exhibit a profound loss of touch sensation. We precisely localize Piezo2 to the peripheral endings of a broad range of low threshold mechanoreceptors (LTMRs) that innervate both hairy and

Reprints and permission information is available at www.nature.com/reprints.

*To whom correspondence should be addressed, ardem@scripps.edu.

†Present address: Ion Channels and Sensory Transduction group, Aix Marseille Université, CNRS, CRN2M-UMR 7286, 13344 Marseille, France.

Author Contributions

SR and AP designed experiments and wrote the manuscript along with GRL. SR, JW and ZQ generated transgenic lines used in this study. SHW performed all immunostaining experiments. AED conducted electrophysiology on cultured DRG neurons and JM isolated and cultured cells. RAM, CW, VB and GRL performed skin nerve electrophysiology and analyzed the data. SR, MP, AGF, KR performed behavioral assays on mice. BC, JM and AJW developed the novel two choice mechanosensory instrument.

The authors declare no competing financial interests.

Supplementary Information is linked to the online version of the paper at www.nature.com/nature.

glabrous skin. Most RA MA currents in DRG neuronal cultures are absent in *Piezo2^{CKO}* mice, and *ex vivo* skin nerve preparation studies show that mechanosensitivity of LTMRs strongly depends on Piezo2. This striking cellular phenotype correlates with an unprecedented behavioral phenotype: an almost complete deficit in light touch sensation in multiple behavioral assays, without affecting other somatosensory functions. Our results highlight that a single ion channel that displays RA MA currents *in vitro* is responsible for the mechanosensitivity of most LTMR subtypes involved in innocuous touch sensation. Interestingly, we find that touch and pain sensation are separable, suggesting that yet-unknown MA ion channel(s) must account for noxious (painful) mechanosensation.

DRG neurons have pseudounipolar axons that terminate in the skin where they form specialized mechanoreceptors that are tuned to detect mechanical forces such as stretch, indentation, and vibration¹. A diverse set of low threshold mechanoreceptors are distributed within hairy and glabrous skin. Lanceolate and circumferential endings that contain a mixed population of A β -, A δ -, and C-LTMRs are specific to hairy skin, whereas various corpuscles that consist of A β RALTMRs are unique to glabrous skin^{1,8}. Merkel cell-neurite complexes that mediate slowly adapting (SA) responses in A β fibers are present in both skin types⁴. These structurally diverse LTMRs together detect mechanical stimuli relevant to innocuous touch sensation.

We had previously shown that Piezo2 was expressed in Merkel cell-neurite complexes and that Merkel cells partly contributed to SA type I Firing (SAM I)^{4,5,9}. Whether Piezo2 was also expressed in other cutaneous mechanoreceptors and whether it functioned as the primary mechanotransduction ion channel was not known. We therefore used a recently generated mouse line, *Piezo2-GFP*, where the Green Fluorescent Protein (GFP) was fused to the C-terminus of *Piezo2*, to detect localization of Piezo2 at the site of mechanical transduction: in the nerve terminals of sensory neurons that project to the skin⁴. In hairy skin, GFP expression was found in both lanceolate endings and circumferential fibers that have varying degrees of myelination and wrap around the bulge region of hair follicles (Figs. 1a and 1b). Consistent with our previous analysis, Piezo2 was expressed in Merkel cells in both hairy skin and glabrous skin (Fig. 1c)^{4,5}. In glabrous skin, Piezo2 was also expressed in Meissner's corpuscles (Fig. 1d). Overall, Piezo2 expression is found in a broad range of LTMRs that sense mechanical stimuli relevant to touch sensation.

Constitutive deletion of *Piezo2* led to perinatal lethality; therefore, we used an inducible strategy to delete *Piezo2* in adult mice¹⁰. The *AvCreERT2* mouse line allowed for tamoxifen-induced activation of Cre recombinase under the Advillin promoter in sensory neurons and in epidermal Merkel Cells¹¹. We first characterized the expression overlap in DRGs between *AvCreERT2* and *Piezo2* by mating the *AvCreERT2* mouse to the *Ai9* tdTomato reporter line. In agreement with a previous report, we found that 87% of total DRG neurons express tdTomato (766/876 total cells) (Fig. 2a). Co-expression analysis of tdTomato epifluorescence with a Piezo2 antibody staining showed that 82% of Piezo2⁺ cells were also tdTomato⁺ (343/419 cells out of 876 total) (Fig. 2a)⁴. We also detected expression of tdTomato in epidermal Merkel cells (data not shown), indicating the *AvCreERT2* mouse line would lead to deletion of *Piezo2* in all cell types either proposed or known to be

relevant to somatosensory transduction¹¹. These data further indicated that while *AvCreERT2* would ablate *Piezo2* in most DRG neurons, a small number of *Piezo2*^{+/Cre} neurons might still remain intact. We then mated the *AvCreERT2* mouse to a previously generated conditional knockout mouse line, *Piezo2*^{flx}, and found that *Piezo2* expression levels were similar between genotypes before tamoxifen injections (Fig. 2b, top). After tamoxifen injections, *Piezo2* immunostaining in *Piezo2*^{CKO} mice showed a marked decrease in number of positive DRG neurons compared to *Piezo2*^{WT} mice (Fig. 2b, bottom) and qPCR analysis revealed a ~90% deletion of overall *Piezo2* transcripts in isolated DRGs (Fig. 2c).

Previous reports had shown that cultured DRG neurons that were transfected with siRNA for *Piezo2* showed a selective decrease in rapidly adapting (RA) MA currents^{3,12}. We determined the sensitivity of cultured DRG neurons from *Piezo2*^{CKO} mice to mechanical indentation using a piezoelectrically-actuated blunt glass probe^{10,13,14}. DRGs from *Piezo2*^{CKO} mice had dramatically fewer neurons with RA whole cell current responses compared to controls (Fig. 2d and Extended Data Fig. 1a), and a corresponding increase in the proportion of mechanically insensitive neurons (NR). There were no significant effects on intermediately adapting (IA) and slowly adapting (SA) currents (Fig. 2d and Extended Data Figs. 1b and 1c), and there were no differences between genotypes for access resistance, membrane resistance, and resting membrane potential (Extended Data Table 1). Interestingly, we observed a wide range of low and high apparent thresholds for RA currents in *Piezo2*^{WT} neurons, while none of the remaining RA responses in *Piezo2*^{CKO} neurons were apparently low threshold (Extended Data Fig. 2). Whether the RA activity in sensory neurons of *Piezo2*^{CKO} mice is mediated by any remaining *Piezo2* or another MA channel is not known. Nonetheless, these results suggest that *Piezo2* accounts for the majority of RA currents in cultured DRG neurons.

In order to confirm that loss of *Piezo2* did not affect the integrity of DRG neurons, we performed immunostaining analyses of DRG neurons using markers of various subpopulations. The expression patterns of Neurofilament heavy polypeptide (Nefh), Thymidine Hydroxylase (TH), and Calcitonin gene-related peptide (CGRP) were unaffected in *Piezo2*^{CKO} DRGs relative to *Piezo2*^{WT} DRGs (Extended Data Figs. 3a-f). Moreover, *Piezo2*^{WT} as well as *Piezo2*^{CKO} mice showed normal cutaneous mechanoreceptor formation including Merkel cell-neurite complexes (Extended Data Figs. 4a and 4d), lanceolate and circumferential endings (Extended Data Figs. 4b, 4e and 4f), and Meissner's corpuscles (Extended Data Figs. 4c and 4g). We also performed calcium imaging in cultured DRG neurons and found no significant differences in the number of capsaicin responsive cells between the two genotypes (data not shown).

Loss of MA currents in cultured DRG neurons is expected to be associated with a loss of mechanosensitivity of sensory fibers in the skin¹⁵. We tested this using an *ex vivo* skin nerve preparation in which mechanically insensitive fibers were identified with an electrical search technique (Extended Data Table 2)^{15,16}. In *Piezo2*^{CKO} mice, 50% of the A β -fibers had no detectable mechanosensitivity compared to less than 10% of A β -fibers from *Piezo2*^{WT} mice (Fig. 3a). There was a non-significant decrease in the proportion of A δ -fibers in *Piezo2*^{CKO} lacking mechanosensitivity, and there was no significant loss of mechanosensitivity in C-

fibers (<10% in both genotypes) (Fig. 3a). Despite the dramatic loss of mechanosensitivity, the axonal conduction velocities of A β -, A δ - and C-fibers were unchanged in *Piezo2^{CKO}* mice compared to controls (Extended Data Fig. 5a).

We also investigated A β -fibers with a mechanosensitive receptive field using a series of ramp and hold force stimuli with ramp phases of different velocities (Figs. 3b and 3c). Slowly-adapting mechanoreceptors associated with Merkel cells (SAM) are known to have a characteristic irregular firing during static displacement and a prominent dynamic discharge during the ramp¹⁷. We showed previously that deletion of *Piezo2* in Merkel cells led to reduced firing in the static phase but not the dynamic phase⁴. Here, most SAMs encountered in *Piezo2^{WT}* (22/31 fibers) and *Piezo2^{CKO}* (7/10 fibers) could be classified as likely SA type I fibers (SAM I) associated with Merkel cells (Extended Data Table 2)^{17,18}. Strikingly, the characteristic dynamic response of SAM I fibers recorded from *Piezo2^{CKO}* mice was almost absent compared to controls with all velocity ramps tested (Fig. 3b-3d); in addition, these fibers displayed drastically reduced static responses. The prominent deficit in A β SA fibers described here is consistent with the hypothesis that *Piezo2* in both Merkel cells and sensory afferents contributes to SAM I firing activity^{4,5}. Rapidly-adapting mechanoreceptors (RAMs) that innervate hair follicles also increase their firing rates with increasing stimulus speed¹⁹. This velocity sensitivity was almost absent in the remaining RAMs encountered in *Piezo2^{CKO}* mutant mice (Fig. 3e).

Examination of the mechanical thresholds and stimulus response functions of A δ - and C-fibers revealed that A δ -mechanonociceptors (A-Ms) exhibited elevated thresholds (Fig. 3f and Extended Data Fig. 5b), but the mechanosensitivity of C-fiber nociceptors were unaffected in *Piezo2^{CKO}* mutant mice (Fig. 3f and Extended Data Fig. 5c).

Mechanoreceptors called D-hairs with A δ -fiber axons were encountered less frequently in *Piezo2^{CKO}* mutant mice compared to controls but this did not reach statistical significance (Fisher's exact test $p > 0.1$) (Extended Data Table 2), but the four fibers encountered showed stimulus response properties indistinguishable from those in controls (Extended Data Fig. 5d). Most C-fibers are polymodal and respond to chemical and thermal stimuli in addition to mechanical pressure. Using a Peltier device, the thermal sensitivity of C-fibers was tested, and both heat threshold for the first spike and the mean firing rates to the standard heat stimulus (ramp 1 °C/s 32-48 °C) were unchanged in *Piezo2^{CKO}* mutant mice compared to controls (Fig. 3g and Extended Data Fig. 5e). Noxious cold sensitivity of *Piezo2^{CKO}* mutant C-fibers was also unaffected (data not shown). We and others have recorded C-fibers with very low mechanical thresholds (C-LTMR) in the hairy skin, but their rarity precluded a detailed analysis as we did not encounter any C-LTMRs in our control sample (Extended Data Table 2).

Our electrophysiological findings from the hairy skin demonstrate that mechanosensitivity of DRG neurons to low threshold forces is by large part mediated by *Piezo2*; however, the mechanosensitivity of most nociceptors is largely unaffected in *Piezo2^{CKO}* mice. Any remaining mechanosensitivity in *Piezo2^{CKO}* A β -fibers could be due to incomplete *Piezo2* ablation in *Piezo2^{CKO}* mice or the presence of yet-unidentified MA ion channels. Our finding of an elevation in the mean mechanical threshold for activation of A δ -mechanonociceptors suggests that *Piezo2* may contribute partly to mechanosensitivity of

these neurons, a finding consistent with recent data indicating that single sensory neurons often possess multiple mechanosensitive currents²⁰.

We next performed a battery of behavioral assays to test innocuous and noxious mechanical and thermal sensitivities of *Piezo2^{CKO}* mice. We tested for the ability of *Piezo2^{CKO}* mice to detect von Frey filaments of varying forces applied to their hind paws²¹. Whereas *Piezo2^{WT}* mice showed a linear increase in detection of von Frey filaments from 1.0g to 5.5g, *Piezo2^{CKO}* mice were severely impaired in their ability to respond to forces below 4.0g (Fig. 4a). Interestingly, *Piezo2^{CKO}* mice showed no differences in sensing the higher forces, highlighting the role of Piezo2 in a specific range of mechanical stimuli and indicating that *Piezo2^{CKO}* mice were able to perform motor functions. We then used the cotton swab assay where a sweeping motion of cotton underneath the mouse paw led to consistent withdrawal responses in *Piezo2^{WT}* mice, whereas *Piezo2^{CKO}* mice showed dramatically reduced responses to the cotton swab stimulus (Fig. 4b)²². We also built a novel two-choice preference assay to evaluate innocuous mechanosensation (Extended Data Figs. 6a and 6b) and found that C57/B16J mice consistently avoided the mechanically active side (Extended Data Fig. 6c)²³. *Piezo2^{WT}* mice behaved similarly to C57/B16J mice and showed a robust avoidance behavior to this stimulus, whereas the *Piezo2^{CKO}* mice showed no preference (Fig. 4c).

In the assays described above, the paws of the mice receive the majority of the mechanical stimulation. We therefore tested the response of *Piezo2^{CKO}* mice to a mechanical stimulus given to hairy skin. We used a modified version of the tape response assay to monitor the response of mice to adhesive tape attached to their back²⁴. *Piezo2^{WT}* mice showed clear responses to the tape and made ~80 attempts to remove the tape over the course of five minutes. *Piezo2^{CKO}* mice barely responded to this stimulus (Fig. 4d). These data demonstrate that *Piezo2^{CKO}* mice have a dramatic inability to sense innocuous touch. Interestingly, when Piezo2 is deleted in epidermal Merkel cells but not in DRG neurons using the *K14-Cre* line, these mice had a slight defect in response to von Frey filaments, but no defects in the other three innocuous touch behavioral assays described here (data not shown)⁴. Importantly, to confirm that this behavior is not due to Piezo2 deletion in non-sensory tissues, we performed immunostaining using the *Piezo2-GFP* reporter mouse line and were unable to detect Piezo2 expression in motor neurons, cerebellum or skeletal muscle (data not shown). Therefore, the considerably more pronounced behavioral deficits resulting from Piezo2 deletion via *AvCreERT2* emphasize the primary role of sensory neurons in touch sensation.

We then asked if *Piezo2^{CKO}* mice were able to respond to thermal stimuli and noxious mechanical forces. *Piezo2^{CKO}* mice showed no differences compared to littermate controls in innocuous temperature sensation, demonstrating that the deficits in mechanical insensitivity are not due to general health issues (Fig. 4e)²³. To determine if *Piezo2^{CKO}* mice could respond to noxious mechanical stimuli, we first used a ramping von Frey protocol and found that *Piezo2^{CKO}* mice showed no differences in threshold for response compared to *Piezo2^{WT}* mice (Extended Data Fig. 7a). These results are in line with the single force von Frey assay where the major deficit was observed only for low threshold stimuli. *Piezo2^{CKO}* mice also showed similar responses to *Piezo2^{WT}* mice in noxious force sensing assays such

as tail clip and Randall-Selitto (Extended Data Figs. 7b and 7c). Furthermore, we observed no differences to noxious temperature sensitivity between control and *Piezo2^{CKO}* mice (Extended Data Fig. 7d). Recent reports have suggested a role for Piezo2 in mechanical allodynia^{12,25}. Although Piezo2 activity is sensitized in response to inflammatory signals *in vitro*, we did not observe any behavioral deficits in mechanical nociception or mechanical allodynia in response to inflammatory mediators in *Piezo2^{CKO}* mice (Extended Data Figs. 7e and 7f)¹⁰. Future studies are needed to explore Piezo2 mechanical sensitivity in response to nerve injury.

Ion channels responsible for detecting mechanical stimuli relevant for somatosensation have been long sought, and our results demonstrate that Piezo2 is the major mechanotransducer required for touch sensation in mammals. The loss of the MEC-2 related protein STOML3 also leads to loss of mechanoreceptor sensitivity^{15,20} and interestingly recent data shows that this protein is a powerful positive modulator of Piezo channel mechanosensitivity²³. We show that Piezo2-dependent RA MA currents *in vitro* account for the mechanosensitivity of the majority of LTMRs without affecting the function of nociceptors. It is interesting that a Piezo2-mediated RA current *in vitro* can account for both RA and SA fiber responses *in vivo*. At least in Merkel cells, the small remaining Piezo2-mediated current during long lasting stimulations is sufficient to produce large sustained depolarization, probably due to the high membrane resistance of these cells, which leads to slowly adapting responses in sensory afferents^{4,5}. Our electrophysiological results are unambiguously supported by behavioral studies that show an almost complete deficit in touch sensation without affecting pain sensation in Piezo2-deficient mice, and predict the existence of other mechanotransducers relevant for pain sensation. Piezo1, a related mechanosensitive ion channel required for vascular development, is not expressed at significant levels in sensory neurons to be a likely candidate (Extended Data Figs. 8a and 8b)²⁶. Ion channels that sense cell volume, such as the recently identified SWELL1 might also play a role in nociception^{27,28}. Furthermore, the yet-unknown cationic channels that account for the IA and SA MA currents in cultured DRGs (Fig. 2d) are likely to be involved in nociception. Different mechanotransducers also account for innocuous and noxious mechanosensation in *Drosophila*². Interestingly, *Drosophila* Piezo is required for mechanical nociception, and not for gentle touch sensation²⁹. Regardless, our findings highlight the role of Piezos as evolutionarily conserved MA ion channels involved in somatosensory mechanotransduction from flies to mammals^{29,30}.

Methods

All animal procedures were approved by TSRI Institutional Animal Care and Use Committees or were approved by the animal welfare office of federal state of Berlin.

Immunofluorescence

Dorsal Root Ganglia Neurons (DRG), dorsal skin, and footpads were collected from 7-week-old mice. Tissues were briefly fixed in 4% PFA and were processed as previously described⁴.

Fluorescent images were captured using a Nikon confocal microscope C2. Antibodies used for immunofluorescence staining were previously reported with the addition of TH (Millipore) and CGRP (Abcam)⁴. Immunostaining images from Ai9 reporter mouse crossed to the *AvCreERT2* Cre line were visualized by tdTomato epifluorescence^{31,32}.

Cell Culture and siRNA of Dorsal Root Ganglia (DRG) Neurons

DRG cultures and transfection of siRNA (for Piezo1 experiments) were performed exactly as previously described³. Reagents: Mouse Piezo1 siRNA smart pool Dharmacon (ONTARGETplus Mouse Piezo1 (234839) siRNA - SMARTpool; Catalog# L-061455-00-0005); Scramble siRNA controls, Qiagen Allstars Negative Control (SI03650318).

In situ hybridization

DRG neurons from C57BL/6J mice were harvested from all levels and fixed in 10% formalin overnight. The DRG neurons were then dehydrated through an ethanol series/ xylene and embedded in paraffin. 10 μ m sections were cut and *in situ* hybridization was carried out using the RNAscope assay (Advanced Cell Diagnostics; Hayward, CA) according to the manufacturer's instructions. Development of signal was done using the RNAscope 2.0 HD brown detection kit. Probes for mPiezo1 (cat number: 400181) and mPiezo2 (cat number: 400191) were purchased from Advanced Cell Diagnostics (Hayward, CA). Slides were mounted with Cytoseal and imaged under a bright field microscope. Slides were scanned and images captured using the Nanozoomer 2.0 HT (Hamamatsu).

Electrophysiology

Whole cell patch clamp recordings were performed as described using standard methods to achieve low access resistance^{4,10}. Cells were maintained at 22-24 °C in (in mM): 127 NaCl, 3 KCl, 1 MgCl₂, 2.5 CaCl₂, 10 dextrose, 10 HEPES (pH 7.3). Electrodes had resistances of 4.6 ± 0.7 M Ω (n=117) when filled with gluconate-based low chloride intracellular solution (in mM): 125 K-gluconate, 7 KCl, 1 CaCl₂, 1 MgCl₂, 10 HEPES, 1 tetraK-BAPTA, 4 Mg-ATP, 0.5 Na-GTP (pH7.3 with KOH). Neurons with diameters of 14 to 41 μ m were tested for mechanosensitivity using a fire-polished glass probe; the average cell diameter was similar among genotypes (23.1 ± 0.8 μ m (n=57) and 22.7 ± 0.7 μ m (n=62), respectively). The probe displacement was advanced in increments of 0.5 or 1 μ m. All data were analyzed as previous described^{3,10}.

Ex vivo skin nerve preparation

The skin-nerve preparation was used essentially as previously described to record from single primary afferents¹⁶. Mice were euthanized by CO₂ inhalation for 2–4 min followed by cervical dislocation. The saphenous nerve and the shaved skin of the hind limb were dissected free and placed in an organ bath at 32°C. The chamber was perfused with a synthetic interstitial fluid (SIF buffer) the composition of which was (in mM): NaCl, 123; KCl, 3.5; MgSO₄, 0.7; NaH₂PO₄, 1.7; CaCl₂, 2.0; sodium gluconate, 9.5; glucose, 5.5; sucrose, 7.5; and HEPES, 10 at a pH of 7.4. The skin was placed with the corium side up in the organ bath. The saphenous nerve was placed in an adjacent chamber on a mirror to aid

and under microscopy fine filaments were teased from the nerve and placed on the recording electrode. Electrical isolation was achieved with mineral oil.

For the electrical search protocol a microelectrode (0.5-1 M Ω) was maneuvered gently to contact the epineurium of saphenous nerve and deliver electrical stimulations at 1-s interval with square pulses of 50-500 ms duration. In most filaments 5-7 single units were encountered. The electrical nerve stimulation was done at up to 3 sites (corresponding to major branching points of the saphenous nerve) to trace electrically identified units to their receptive fields. Mechanical sensitivity of single units was tested by mechanical stimulation of their receptive field with a glass rod; units not responding to mechanical probing were designated as mechano I /N-sensitive. Based on the conduction velocity, these units were categorized as mechanically insensitive A β , A δ , and C-fibers.

Mechanically sensitive units were characterized by conduction velocity (calculated by dividing conduction distance over electrical latency for the spike) and stimulus response function was obtained by a standardized mechanical stimulation protocol. The stimulating probe, equipped with a force transducer (Kleindiek, Reutlingen, Germany), was placed onto a spot within the receptive field where the most reliable responses could be obtained. The probe was a stainless steel metal rod and the diameter of the flat circular contact area was 0.8 mm. Two mechanical stimulation protocols were employed. The first stimulation protocol was applied to SAM, RAM, and D-hair receptors. A piezo actuator (Physik Instrumente) was used to deliver 5 ramp and hold stimuli (90 μ m displacement, 2 s hold-phase, and 30 s interstimulation interval) with increasing ramp velocities (0.075, 0.15, 0.45, 1.5, and 15 mm/s). The second stimulation protocol was applied to A-M and C-fibers and consisted of an ascending series (6 ramp and hold stimuli) of 10 s displacement stimuli (32 -1024 μ m) at 30 s intervals, sent as a preprogrammed series of commands to a computer-controlled nanomotor (Kleindiek, Reutlingen, Germany). Mechanical thresholds for nociceptors were measured by reading off the force (obtained from the attached force transducer) at which the first spike was obtained. The signal driving the movement of the linear motor and raw electrophysiological data were collected with a Powerlab 4.0 system (ADInstruments) and spikes were discriminated off-line with the spike histogram extension of the software. Data was obtained from between 6 and 20 skin nerve preparations per genotype.

Tamoxifen injections

15 mg of tamoxifen (Sigma) was dissolved into 1 ml of 100% Corn Oil and made fresh daily before use. *Piezo2*^{WT} and *Piezo2*^{CKO} mice both received tamoxifen injections (i.p.) at 150 mg/kg for 5 consecutive days. Due to variability in tamoxifen injections and the observation of incomplete deletion in *Piezo2*^{flx/flx} mice, *Piezo2*^{flx/-} mice, containing one floxed allele and one null allele, were used for analysis. *Piezo2*^{CKO} refers to mice that received tamoxifen injections. Each mouse was weighed before injection to normalize for differences in body weight. Somatosensory behavioral assays were performed on mice between 7 and 21 days after tamoxifen injections, and all mice that were tested for mechanical sensitivity were also tested for thermal sensitivity to control for any issues of general health. Before tamoxifen injections, *Piezo2*^{CKO} mice were healthy and viable with no differences compared to

Piezo2^{WT} littermate controls in various somatosensory assays (data not shown). However, tamoxifen injections led to a visible difference in behavior of *Piezo2*^{CKO} but not *Piezo2*^{WT} mice that started ~7 days after the last injection. *Piezo2*^{CKO} mice walked with an irregular gait, sometimes dragged their hind legs, and were occasionally uncoordinated when attempting to stand on their hind legs.

Quantitative Real Time PCR (qPCR) analysis

qPCR analysis was performed by first isolating total RNA using Trizol/Chloroform and isopropanol precipitation from freshly isolated DRG neurons (Life Technologies). Generation of cDNA was achieved by Reverse Transcription using the QuantiTect Reverse Transcript Kit (Qiagen). For qPCR, FastStart Universal probe master mix (Rox) from Roche Diagnostics was used. The reaction was run in the Eco Real-Time PCR instrument (Illumina) using 0.5 ul of the cDNA in a 10 ul reaction according to the manufacturer's instructions. Real time Taqman qPCR assays were purchased from Integrated DNA Technologies with a FAM reporter dye and a non-fluorescent quencher: mouse *Piezo2* (Mm.PT.56a.32860700, Fam38b), and an internally designed mouse *Gapdh* assay (forward primer- GCACCACCAACTGCTTAG; reverse primer- GGATGCAGGGATGATGTTC and probe- CAGAAGACTGTGGATGGCCCCTC).

Calibrations and normalizations were done using the $2^{-\Delta\Delta C_T}$ method, where $\Delta\Delta C_T = ((C_T(\text{target gene}) - C_T(\text{reference gene})) - (C_T(\text{calibrator}) - C_T(\text{reference gene})))$. *Gapdh* was used as the reference gene for all qPCR experiments³³.

Static Force von Frey

Responses to application of a von Frey filament was performed as previously described^{21,34}. Mice are acclimated in an elevated platform for 1 hour, in a similar manner to that described for the cotton swab assay. A Dynamic Plantar Aesthesiometer is used to apply varying forces of a 0.5 mm von Frey filament (Ugo Basile product ID 37450). A single force is applied for one second to the hind paw and a yes/no withdrawal response is scored. Forces on the instrument are measured with units “g” and represent grams-force, according to manufacturer's description (Ugo Basile). The initial force applied is 5.5 g and is lowered incrementally by 0.5 g, and testing ends after reaching 1.0g. The fraction of the number of responses out of four applications per force is measured. Data are plotted as percentage of withdrawal at each force for control and test mice.

Two Choice Mechanosensory Assay

The novel two choice mechanosensory assay instrument consists of two lightweight, stiff, composite platforms which are separately activated by a pair of tactile transducers (Clark Instruments). The platforms are mounted to the frame via low rate coil springs. The springs act to mechanically isolate the platforms from each other and the frame. A thin sheet of silicone rubber is fastened to the tops of the platforms and the frame. This provides a continuous surface that covers the gaps between the frame and platforms. Dividers are placed on top of the frame to create the lanes. A clear plastic cover sits on all lanes in order to prevent mice from climbing out of the lane. Tactile transducers housed underneath the

platforms are connected to a 2 channel amplifier which is fed the appropriate sine wave signals via a Labview controlled signal generator.

For behavioral analysis, individual mice were placed in one of 6 lanes, with a maximum of 6 mice tested at the same time. We optimized the output of the stimulator using multiple protocols and found that C57/B16J mice consistently avoided the active side when using a protocol of 150 Hz (sine wave), at a peak to peak displacement of 33.1 μm and a pulsing stimulus of 3 seconds on and 2 seconds off. Interestingly, mice showed decreased avoidance of the active side when the vibration stimulus was kept constant. A side at random was turned off and the other side was turned on to a pulsing stimulus. The acceleration and frequency produced were monitored using a custom designed program (Dual Channel v.7) to ensure only one side was active. Mice were allowed to walk freely between two zones for ten minutes with no stimulus and were assayed for 1 hour with the pulsing protocol. EthoVision tracking system (Noldus Information Technology) was used to monitor the movement of the mice in a dark room illuminated with IR light. Data are plotted as % of the time spent on the active zone.

Cotton Swab Assay

A method to assess light touch evoked paw withdrawal was used as described previously²². Mice were placed in an elevated acclimation chamber separated by plexiglass dividers. The floor consists of mesh-like grids that are accessible from below due to small gaps of $\sim 5 \times 5$ mm (Ugo Basile product ID 37450-277). Mice are allowed to acclimate for 1 hour before testing. A cotton swab from a Q-tip is manually pulled so that it is “puffed out” to $\sim 3 \times$ the original size. A sweeping motion, rather than an upward motion, is used underneath the mouse paw and mice are assayed for a paw withdrawal response. Five sweeps are performed with at least 10 seconds between each sweep. The number of withdrawals out of 5 times are counted and recorded as a percentage (%) for each mouse.

Tape Response Assay

A modified version of the tape on paw assay was performed²⁴. Mice are allowed to acclimate in a circular plexiglass container for 5 minutes. A 3 cm piece of common lab tape was then applied gently to the back of the mouse such that it sticks to the mouse. Mice are then observed for 5 minutes and the total number of responses to the tape are counted. A response is scored when the mouse stops moving and bites or scratches the piece of tape or shows a visible “wet dog shake” motion in an attempt to remove the foreign object on its back.

Ramping von Frey

Responses to an application of increasing, ramping, force von Frey filament was performed as previously described²¹. Mice are acclimated and tested using the same Dynamic Plantar Aesthesiometer described for single force von Frey (Ugo Basile). Instead of a single force application, a ramping protocol is used that increases in force from 0-50 g over the course of 20 seconds. The Von Frey filament is applied until the mouse withdraws its hind paw. Each mouse receives four applications of the von Frey filament and the average force (threshold for withdrawal) is plotted for each mouse.

Hargreaves Assay

A paw withdrawal response to an IR20 light is performed as previously described²¹. Mice are allowed to acclimate on a plexiglass container with a clear flat bottom for at least 60 minutes. The heat source for IR light is set to intensity 20 (Ugo Basile product ID 37300). The heat source is placed under the platform where mice are acclimated and the light is applied to the hind paw. The time to paw withdrawal is measured and repeated 3 times for each mouse with a cutoff of 20 seconds. The average time to withdrawal is plotted (latency) for each mouse.

Randall-Selitto Assay

Response to a noxious level of pinching force on the paw of a mouse was performed as previously described³⁴. Mice are placed into a small sling that allows the mice to be restrained and the paws to be accessible (IITC Life Sciences). A pinching force application is given to the hind paw using a Randall-Selitto device (IITC Life Sciences). Three separate pinches are applied where the force increases until reaching a 300g cutoff. A response is scored by any visible flinch or audible vocalization. Data are plotted as the average of three responses (threshold) calculated for each mouse.

Tail Clip Assay

An assay to determine the time for response to an alligator clip placed on the tail of a mouse was slightly modified from³⁵. An alligator clip commonly used for electrical wires was purchased from The Home Depot. The clips were altered by filing down the sharp teeth and then covered with a rubber casing to reduce potential for tissue damage. We calibrated the strength of the force exerted by the clips to be 500 g. The clips were marked at the center to ensure placement of the clip was similar for all mice tested. The clips are placed near the base of the mouse tail and then the mice are placed on a table inside a plexiglass container. A response was scored when the mice showed awareness of the clip by biting, vocalization, grasping of tail or a jumping response. Data are plotted as the time to respond (latency) for each mouse.

Complete Freund's Adjuvant (CFA) Von Frey

A standard assay for inflammation due to Complete Freund's Adjuvant (CFA) injection in the hindpaw was performed as previously described²¹. Mice were subjected to Ramping von Frey (detailed above) before injection of CFA. After baseline analysis, mice were injected in the hind paw with 10 μ l of CFA (Sigma). Mice were then re housed in their home cages and tested by ramping Von Frey the following day, 24 hours post injection.

Bradykinin (BK) Von Frey

Inflammation response to bradykinin (BK) injection was performed as previously described²¹. Animals were acclimated and tested by ramping Von Frey (detailed above). After baseline analysis was performed, mice were then injected with 20 μ l of BK (10 nM). Mice were then placed back in the acclimation chambers and tested by ramping Von Frey at 5, 10 and 15 minutes post injection.

Two temperature choice assay

A preference assay between 32°C and 18°C was performed as previously described²³. Mice were placed on a platform where plexiglass dividers separated the entire platform into six lanes. The platform was divided into two zones such that one side was heated to 32°C and the other side was cooled to 18°C. One mouse was placed per lane and allowed to walk freely between two zones for one hour. An automated tracking device (Noldus Ethovision software) monitored the movement of the mice in a dark room illuminated with IR light. Data are plotted as % of the time spent on 32°C zone vs. 18°C zone.

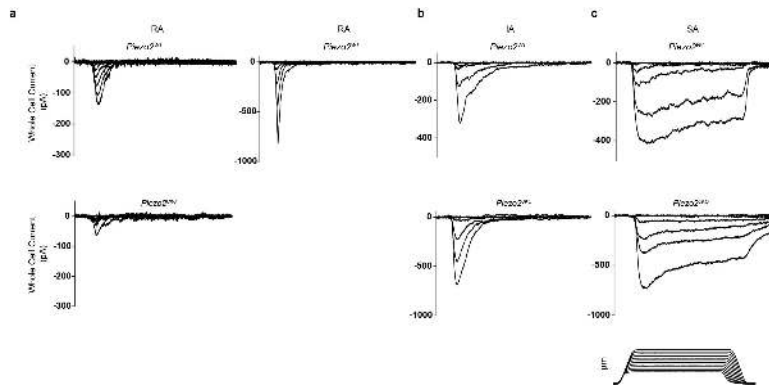
Statistics

All data analyzed by statistical analyses are detailed in the figure legends. Data from electrophysiological analysis and qPCR of isolated DRG experiments were analyzed by Student's t test as previous described³. Electrophysiological skin nerve data were analyzed using Fischer's exact test, Figure 3a; Mann-Whitney test, Figures 3f, g, h; and repeated measures ANOVA, figure 3d, e. For all behavioral experiments, the Mann-Whitney non parametric statistical test was used.

Sample size choice

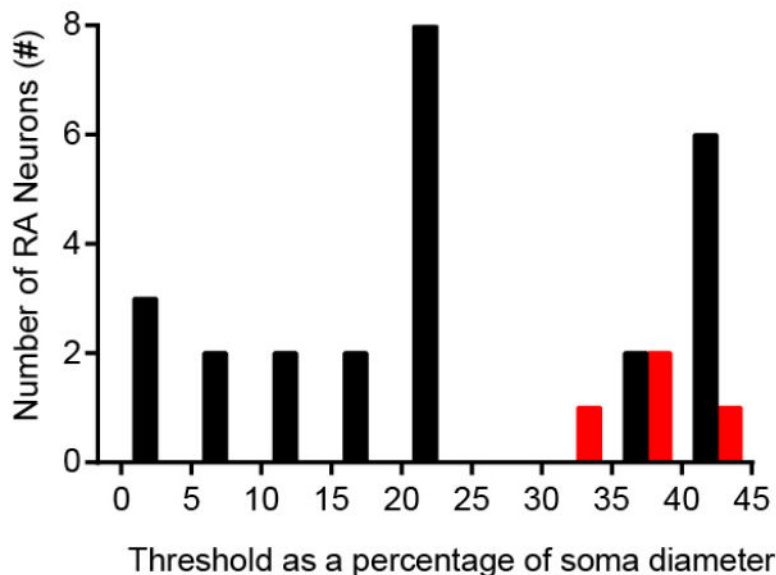
The specific number of independent experiments or animal numbers used for all experiments are outlined in the corresponding figure legends. For electrophysiology and qPCR of DRG experiments, data were analyzed from n = 3 independent experiments. For skin nerve preparations data was obtained from between 6 and 20 skin nerve preparations per genotype. All behavioral data represent results from 2-4 independent rounds of testing with multiple mice of both genotypes per cohort. All mice tested in behavioral assays were littermate controls. All sample choices were chosen in order to ensure significance in statistical assays.

Extended Data

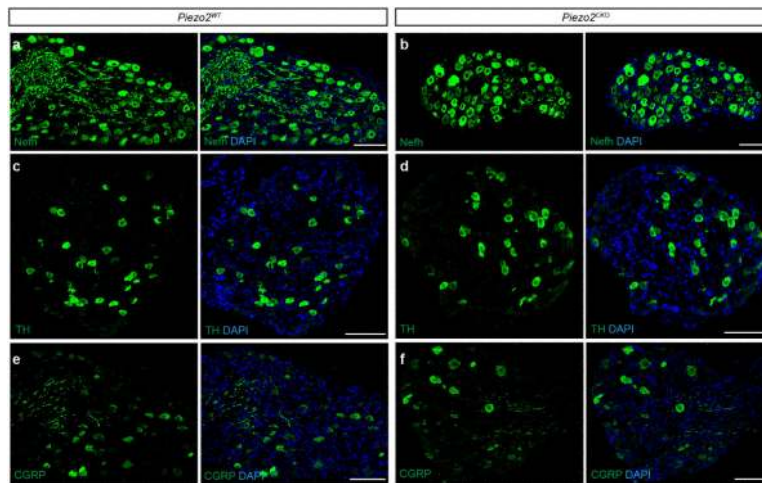


Extended Data Figure 1. MA currents elicited in cultured DRG neurons from *Piezo2*^{WT} and *Piezo2*^{CKO} mice by poking with a blunt probe
a, Representative traces of RA currents in *Piezo2*^{WT} (top) and *Piezo2*^{CKO} (bottom). *Piezo2*^{WT} DRG neurons show characteristic RA currents; a subpopulation can be active with apparent low thresholds (right). *Piezo2*^{CKO} mice contained a few RA type cells but none

were apparent low threshold mechanoreceptors. **b and c**, Representative traces of IA and SA currents, respectively, with no observable differences between the two genotypes. All data were low-pass filtered off line at 4KHz. Action potentials were elicited by current injection in all neurons. *Piezo2^{WT}*: RA, left: 20 μ m diameter, 5 μ m apparent threshold; RA, right: 28 μ m diameter, 1 μ m apparent threshold; IA: 23 μ m diameter, 6 μ m apparent threshold; SA: 20 μ m diameter; 2 μ m apparent threshold. *Piezo2^{CKO}*: RA, left: 23 μ m diameter, 8 μ m apparent threshold; RA, right: none found; IA: 20 μ m diameter, 5.5 μ m apparent threshold; SA: 30 μ m diameter, 8 μ m apparent threshold. Lower right: example of probe displacement protocol (stimulus).

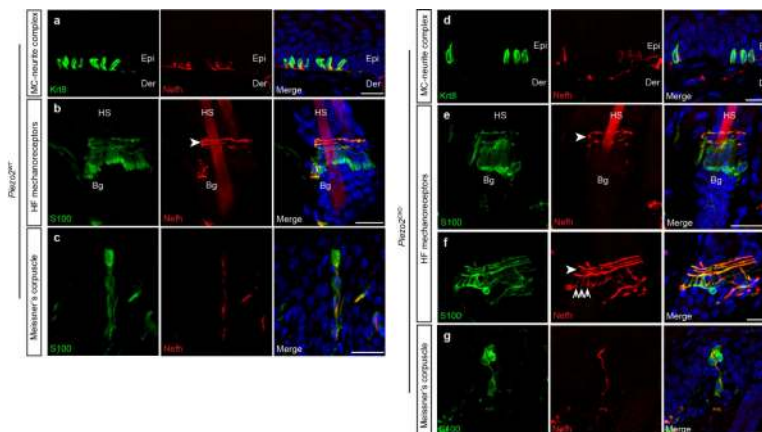


Extended Data Figure 2. Apparent threshold analysis of *Piezo2^{WT}* and *Piezo2^{CKO}* DRG neurons
 The smallest soma indentation eliciting a detectable MA response (apparent threshold) depends, in part, on the incremental distance applied (0.5 μ m) and the proportional displacement in relation to the soma diameter. The apparent thresholds of all RA responses normalized to soma diameter reveal a wide range of sensitivities of *Piezo2^{WT}* DRG neurons (black) and the apparent high threshold responses of the remaining RA neurons in *Piezo2^{CKO}* DRG neurons (red). The lowest apparent thresholds are observed only in *Piezo2^{WT}*.



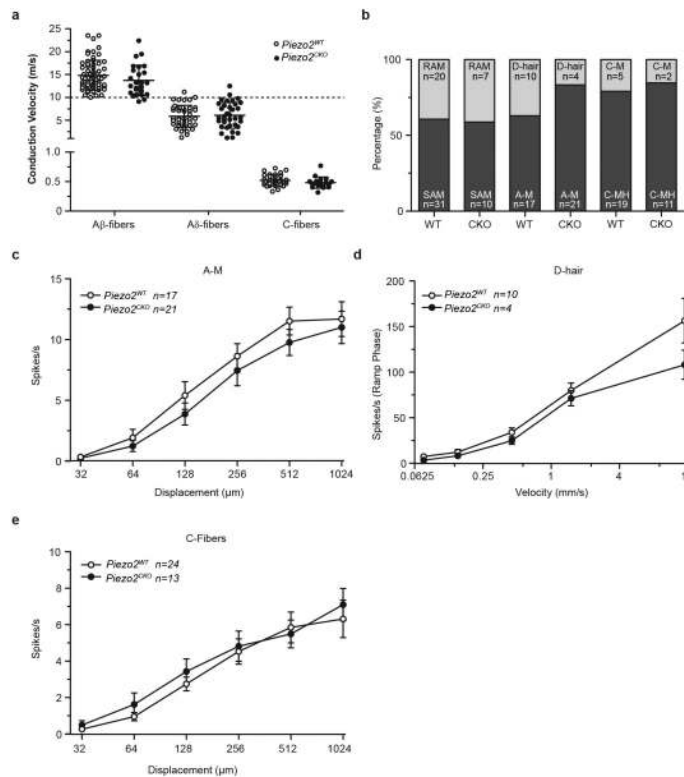
Extended Data Figure 3. Expression of various markers of subpopulations of DRG neurons are similar in *Piezo2*^{WT} and *Piezo2*^{CKO} mice

a and b, Representative images from immunofluorescence of Nefh in DRGs from *Piezo2*^{WT} (a) or *Piezo2*^{CKO} (b) mice. **c and d**, Representative image from immunofluorescence of TH in DRGs from *Piezo2*^{WT} (c) or *Piezo2*^{CKO} (d) mice. **e and f**, Representative image from immunofluorescence of CGRP in DRGs from *Piezo2*^{WT} (e) or *Piezo2*^{CKO} (f) mice. All markers stained in green. Scale bars (A-F) 100µm.



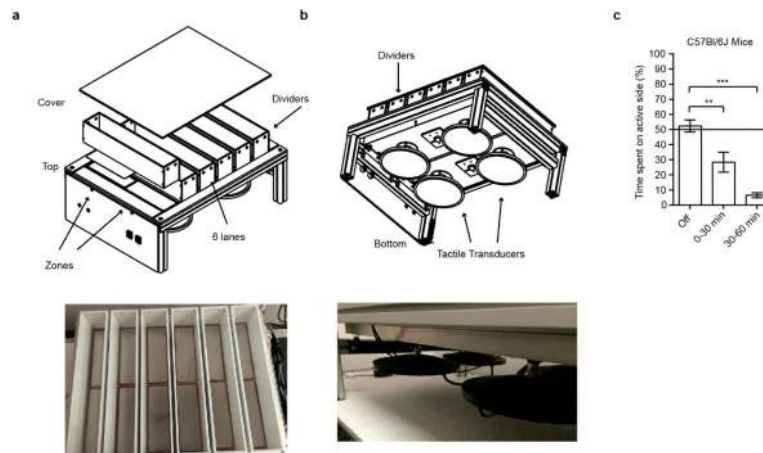
Extended Data Figure 4. DRG innervation of skin is unaffected in *Piezo2*^{CKO} mice

a and d, Representative image of immunostaining of Krt8 (green) and Nefh (red) in Merkel cell - neurite complexes in *Piezo2*^{WT} (a) and *Piezo2*^{CKO} (d) glabrous skin. **b, e and f**, Representative image of immunostaining of S100 (green) and Nefh (red) in circumferential fibers (arrowheads) and lanceolate endings (arrows) in the hair follicle of *Piezo2*^{WT} (b) and *Piezo2*^{CKO} dorsal skin (e and f). **c and g**, Representative image of immunostaining of S100 (green) and Nefh (red) in Meissner's corpuscles in *Piezo2*^{WT} (c) and *Piezo2*^{CKO} (g) glabrous skin. HS, hair shaft; Bg, bulge of the hair follicle; Epi, epidermis; Der, dermis. Scale bars (a-g) 20µm.

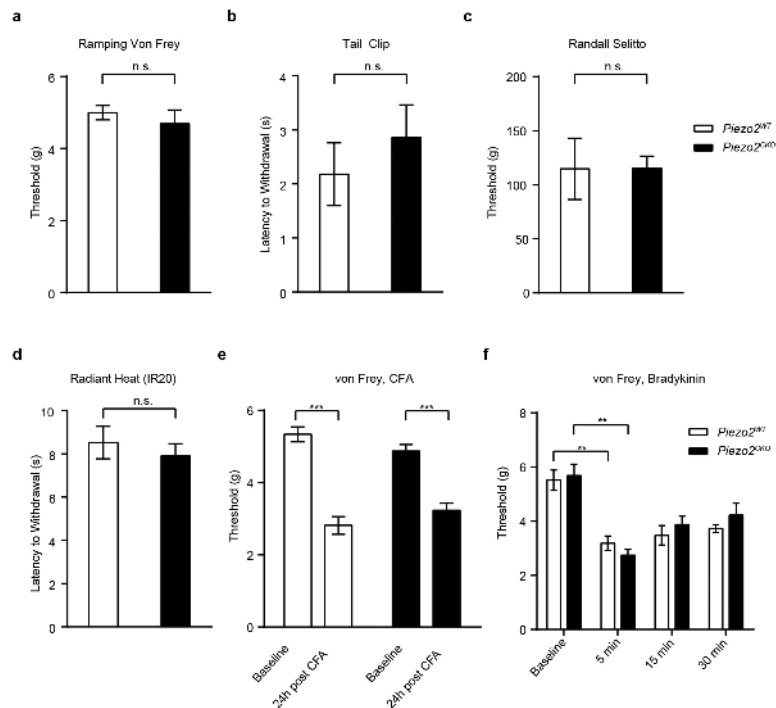


Extended Data Figure 5. Physiological properties of nociceptors are unaffected in *Piezo2^{CKO}* mice

a, No change in conduction velocities of A β -, A δ - and C-fiber afferents in *Piezo2^{CKO}* compared *Piezo2^{WT}* (Mann-Whitney Test). **b**, Proportions of receptor types encountered amongst A β -, A δ - and C-fibers are shown. **c**, Stimulus response properties of A-fiber mechano-nociceptors (A-Ms) recorded in *Piezo2^{CKO}* compared to *Piezo2^{WT}* were not significantly different. **d**, D-hair receptors recorded from *Piezo2^{CKO}* displayed stimulus response properties that were indistinguishable from control afferents. **e**, The stimulus response properties of C-fibers in *Piezo2^{CKO}* were not significantly different from C-fibers recorded in control *Piezo2^{WT}* mice. Data are presented as mean \pm SEM, analysis for c-e with repeated measures ANOVA.



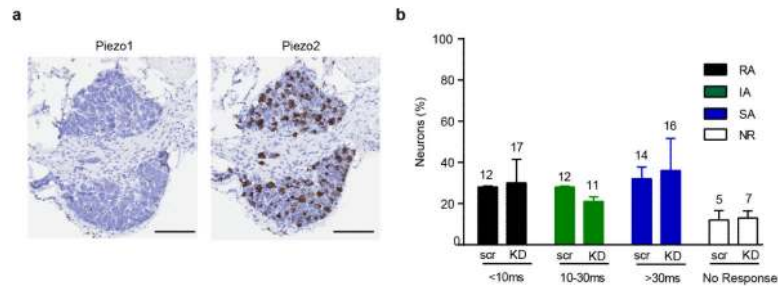
Extended Data Figure 6. Development of Novel Two Choice Mechanosensory Assay
a, Schematic of instrument construction and image of instrument from top angle. **b**, Schematic of the instrument from the bottom angle, with the top cover removed, and photo of tactile transducers underneath the platform. **c**, Avoidance behavior of C57/Bl6J mice to the mechanically active side. Error bars represent SEM, $n = 12$ mice (**c**), 6 males and 6 females. ** $P < 0.005$, *** $P < 0.0001$, Mann Whitney non parametric analysis.



Extended Data Figure 7. *Piezo2*^{CKO} mice do not show deficits in noxious mechanical or thermal stimuli or in inflammatory pain responses

a, Threshold for withdrawal response to a ramping protocol of Von Frey stimulation from low force to high in *Piezo2*^{WT} ($n = 9$) and *Piezo2*^{CKO} ($n = 7$) mice. **b**, Time to response (latency) to application of a 500g tail clip to the base of the tail in *Piezo2*^{WT} ($n = 6$) and *Piezo2*^{CKO} ($n = 7$) mice. **c**, Threshold for response to a Randall-Selitto pinching stimulus to

the hind paw in *Piezo2*^{WT} (n = 5) and *Piezo2*^{CKO} (n = 7) mice. **d**, Time need to withdraw hind paw to an IR20 light (Hargreaves assay) in *Piezo2*^{WT} (n = 13) and *Piezo2*^{CKO} (n = 9) mice. **e**, ramping Von Frey protocol in baseline (before CFA injection) and 24 post CFA injection in *Piezo2*^{WT} (n = 11) and *Piezo2*^{CKO} (n = 9) mice. **f**, ramping Von Frey protocol in baseline (before BK injection) and at time points 5, 15, 15 minutes post injection in *Piezo2*^{WT} (n=6) and *Piezo2*^{CKO} (n=6) mice. Error bars represent SEM, all experiments performed with at least n = 2 separate cohorts of both male and female mice, ** P < 0.005, *** P < 0.0001, Mann Whitney non parametric analysis.



Extended Data Figure 8. Piezo1 expression and function in DRGs

a, *in situ* hybridization expression analysis of Piezo1 in DRG neurons relative to Piezo2. Robust expression of Piezo2 but not Piezo1 is observed, and this agrees with previously reported results using qPCR³. **b**, siRNA for Piezo1 in cultured DRG neurons does not affect the number of mechanically sensitive neurons or ratio of RA, IA or SA type currents (number of recorded neurons in each category indicated on top of bar graphs). Data from n = 3 independent preparations, n.s. by Student's *t*-test). Scale bar: 100 μ m (a).

Extended Data Table 1
 Properties of *Piezo2^{WT}* and *Piezo2^{CKO}* from electrical recordings of cultured DRG neurons.

| Properties | <i>Piezo2^{WT}</i> | <i>Piezo2^{CKO}</i> |
|---------------------------------|----------------------------|-----------------------------|
| Membrane Resistance (MΩ) | 985 ± 140 (n=57) | 860 ± 110 (n=62) |
| Access resistance, Ra (MΩ) | 12.3 ± 0.5 (n=62) | 12.7 ± 0.6 (n=57) |
| Holding current at -80mV (pA) | -272 ± 42 (n=57) | -235 ± 34 (n=62) |
| Resting membrane potential (mV) | -49.3 ± 0.9 (n=57) | -47.8 ± 1.1 (n=62) |
| Rheobase (pA) | 430 ± 90 (57) | 220 ± 35 (60) [*] |
| Number of AP at 2x rheobase | 1.2 ± 0.1 (54) | 1.2 ± 0.1 (59) |
| APD (msec) | 2.45 ± 0.18 (57) | 2.49 ± 0.15 (61) |
| APD range | 0.4, 6 | 0.6, 5.2 |
| AP overshoot (mV) | 71.9 ± 1.6 (57) | 70.7 ± 1.6 (61) |

Values are mean ± SEM (number of neurons). AP, action potential

Student's t-test. This difference is dependent on 8 *Piezo2^{WT}* vs 4 *Piezo2^{CKO}*

^{*} p<0.05

Extended Data Table 2

Properties of single fibers recorded from *Piezo2^{WT}* and *Piezo2^{CKO}* using the saphenous nerve *ex vivo* skin nerve preparation.

| a | |
|--------------------------|--|
| Subclass | <i>Piezo2^{WT}</i> <i>Piezo2^{CKO}</i> |
| A β -fibers | |
| SAM I | 22 7 |
| SAM II | 9 3 |
| RAM | 20 7 |
| A δ -fibers | |
| D-Hair | 10 4 |
| A-M | 17 21 |
| C-fibers | |
| C-LT | - - |
| C-M | 5 2 |
| C-MH | 15 8 |
| C-MHC | 4 3 |
| b | |
| | <i>Piezo2^{WT}</i> <i>Piezo2^{CKO}</i> |
| Mechanically Sensitive | 84 58 |
| Mechanically Insensitive | 4 13 |

a, mechanical search protocol and **b**, electrical search protocol. Definitions as follows C-LT, C-fiber with low threshold mechanosensitivity; C-M, C-mechano-nociceptor only responding to mechanical stimulation and not noxious cold or heat; C-MH, C-mechano heat, responding both to noxious heat and mechanical stimuli; C-MHC, C-mechano heat/cold fiber responding to noxious mechanical heat and cold. Note that small discrepancies between the numbers of fibers listed here and those tested with the full series of mechanical stimuli are due to technical issues preventing full characterization of the unit.

Supplementary Material

Refer to Web version on PubMed Central for supplementary material.

Acknowledgements

We acknowledge Taryn Goode for help in behavioral analysis. We also thank Rita Moran and Terri Johnson for assistance with histology, Kathy Spencer for imaging analysis and Maria Braunschweig for technical assistance. SR was funded by a pre-doctoral fellowship from the California Institute of Regenerative Medicine (CIRM). RAM was supported by Clinical Research Fellowship from the MDC. GRLs lab was supported by senior European Research Council grant (project 294678) and a grant from the Deutsche Forschungsgemeinschaft (SFB958 project A9). AP is a Howard Hughes Medical Institute Investigator. This study was partly funded by NIH grant R01 DE022358 to AP.

References

1. Abraira VE, Ginty DD. The sensory neurons of touch. *Neuron*. 2013; 79:618–639. doi:10.1016/j.neuron.2013.07.051. [PubMed: 23972592]
2. Arnadottir J, Chalfie M. Eukaryotic mechanosensitive channels. *Annu Rev Biophys*. 2010; 39:111–137. doi:10.1146/annurev.biophys.37.032807.125836. [PubMed: 20192782]
3. Coste B, et al. Piezo1 and Piezo2 are essential components of distinct mechanically activated cation channels. *Science*. 2010; 330:55–60. doi:10.1126/science.1193270. [PubMed: 20813920]
4. Woo SH, et al. Piezo2 is required for Merkel-cell mechanotransduction. *Nature*. 2014 doi:10.1038/nature13251.
5. Maksimovic S, et al. Epidermal Merkel cells are mechanosensory cells that tune mammalian touch receptors. *Nature*. 2014 doi:10.1038/nature13250.
6. Ikeda R, et al. Merkel cells transduce and encode tactile stimuli to drive abeta-afferent impulses. *Cell*. 2014; 157:664–675. doi:10.1016/j.cell.2014.02.026. [PubMed: 24746027]
7. Maricich SM, Morrison KM, Mathes EL, Brewer BM. Rodents rely on Merkel cells for texture discrimination tasks. *J Neurosci*. 2012; 32:3296–3300. doi:10.1523/JNEUROSCI.5307-11.2012. [PubMed: 22399751]
8. Lechner SG, Lewin GR. Hairy sensation. *Physiology (Bethesda)*. 2013; 28:142–150. doi:10.1152/physiol.00059.2012. [PubMed: 23636260]
9. Maksimovic S, Baba Y, Lumpkin EA. Neurotransmitters and synaptic components in the Merkel cell-neurite complex, a gentle-touch receptor. *Ann N Y Acad Sci*. 2013; 1279:13–21. doi:10.1111/nyas.12057. [PubMed: 23530998]
10. Dubin AE, et al. Inflammatory signals enhance piezo2-mediated mechanosensitive currents. *Cell Rep*. 2012; 2:511–517. doi:10.1016/j.celrep.2012.07.014. [PubMed: 22921401]
11. Haeberle H, et al. Molecular profiling reveals synaptic release machinery in Merkel cells. *Proc Natl Acad Sci U S A*. 2004; 101:14503–14508. doi:10.1073/pnas.0406308101. [PubMed: 15448211]
12. Lou S, Duan B, Vong L, Lowell BB, Ma Q. Runx1 controls terminal morphology and mechanosensitivity of VGLUT3-expressing C-mechanoreceptors. *J Neurosci*. 2013; 33:870–882. doi:10.1523/JNEUROSCI.3942-12.2013. [PubMed: 23325226]
13. McCarter GC, Reichling DB, Levine JD. Mechanical transduction by rat dorsal root ganglion neurons in vitro. *Neurosci Lett*. 1999; 273:179–182. [PubMed: 10515188]
14. Hu J, Lewin GR. Mechanosensitive currents in the neurites of cultured mouse sensory neurones. *J Physiol*. 2006; 577:815–828. doi:10.1113/jphysiol.2006.117648. [PubMed: 17038434]
15. Wetzel C, et al. A stomatin-domain protein essential for touch sensation in the mouse. *Nature*. 2007; 445:206–209. doi:10.1038/nature05394. [PubMed: 17167420]
16. Moshourab RA, Wetzel C, Martinez-Salgado C, Lewin GR. Stomatin-domain protein interactions with acid-sensing ion channels modulate nociceptor mechanosensitivity. *J Physiol*. 2013; 591:5555–5574. doi:10.1113/jphysiol.2013.261180. [PubMed: 23959680]
17. Maricich SM, et al. Merkel cells are essential for light-touch responses. *Science*. 2009; 324:1580–1582. doi:10.1126/science.1172890. [PubMed: 19541997]

18. Wellnitz SA, Lesniak DR, Gerling GJ, Lumpkin EA. The regularity of sustained firing reveals two populations of slowly adapting touch receptors in mouse hairy skin. *J Neurophysiol.* 2010; 103:3378–3388. doi:10.1152/jn.00810.2009. [PubMed: 20393068]
19. Rugiero F, Drew LJ, Wood JN. Kinetic properties of mechanically activated currents in spinal sensory neurons. *J Physiol.* 2010; 588:301–314. doi:10.1113/jphysiol.2009.182360. [PubMed: 19948656]
20. Poole K, Herget R, Lapatsina L, Ngo HD, Lewin GR. Tuning Piezo ion channels to detect molecular-scale movements relevant for fine touch. *Nat Commun.* 2014; 5:3520. doi:10.1038/ncomms4520. [PubMed: 24662763]
21. Petrus M, et al. A role of TRPA1 in mechanical hyperalgesia is revealed by pharmacological inhibition. *Mol Pain.* 2007; 3:40. doi:10.1186/1744-8069-3-40. [PubMed: 18086313]
22. Garrison SR, Dietrich A, Stucky CL. TRPC1 contributes to light-touch sensation and mechanical responses in low-threshold cutaneous sensory neurons. *J Neurophysiol.* 2012; 107:913–922. doi:10.1152/jn.00658.2011. [PubMed: 22072513]
23. Dhaka A, et al. TRPM8 is required for cold sensation in mice. *Neuron.* 2007; 54:371–378. doi:10.1016/j.neuron.2007.02.024. [PubMed: 17481391]
24. Bradbury EJ, et al. Chondroitinase ABC promotes functional recovery after spinal cord injury. *Nature.* 2002; 416:636–640. doi:10.1038/416636a. [PubMed: 11948352]
25. Eijkelkamp N, et al. A role for Piezo2 in EPAC1-dependent mechanical allodynia. *Nat Commun.* 2013; 4:1682. doi:10.1038/ncomms2673. [PubMed: 23575686]
26. Ranade SS, et al. Piezo1, a mechanically activated ion channel, is required for vascular development in mice. *Proc Natl Acad Sci U S A.* 2014; 111:10347–10352. doi:10.1073/pnas.1409233111. [PubMed: 24958852]
27. Voss FK, et al. Identification of LRRC8 heteromers as an essential component of the volume-regulated anion channel VRAC. *Science.* 2014; 344:634–638. doi:10.1126/science.1252826. [PubMed: 24790029]
28. Qiu Z, et al. SWELL1, a plasma membrane protein, is an essential component of volume-regulated anion channel. *Cell.* 2014; 157:447–458. doi:10.1016/j.cell.2014.03.024. [PubMed: 24725410]
29. Kim SE, Coste B, Chadha A, Cook B, Patapoutian A. The role of *Drosophila* Piezo in mechanical nociception. *Nature.* 2012; 483:209–212. doi:10.1038/nature10801. [PubMed: 22343891]
30. Faucherre A, Nargeot J, Mangoni ME, Jopling C. piezo2b regulates vertebrate light touch response. *J Neurosci.* 2013; 33:17089–17094. doi:10.1523/JNEUROSCI.0522-13.2013. [PubMed: 24155313]
31. Madisen L, et al. A robust and high-throughput Cre reporting and characterization system for the whole mouse brain. *Nat Neurosci.* 2010; 13:133–140. doi:10.1038/nn.2467. [PubMed: 20023653]
32. Lau J, et al. Temporal control of gene deletion in sensory ganglia using a tamoxifen inducible Advillin-Cre-ERT2 recombinase mouse. *Mol Pain.* 2011; 7:100. doi:10.1186/1744-8069-7-100. [PubMed: 22188729]
33. Livak KJ, Schmittgen TD. Analysis of relative gene expression data using real-time quantitative PCR and the 2⁻(Delta Delta C(T)) Method. *Methods.* 2001; 25:402–408. doi:10.1006/meth.2001.1262. [PubMed: 11846609]
34. Kwan KY, et al. TRPA1 contributes to cold, mechanical, and chemical nociception but is not essential for hair-cell transduction. *Neuron.* 2006; 50:277–289. doi:10.1016/j.neuron.2006.03.042. [PubMed: 16630838]
35. Lariviere WR, et al. Heritability of nociception. III. Genetic relationships among commonly used assays of nociception and hypersensitivity. *Pain.* 2002; 97:75–86. [PubMed: 12031781]

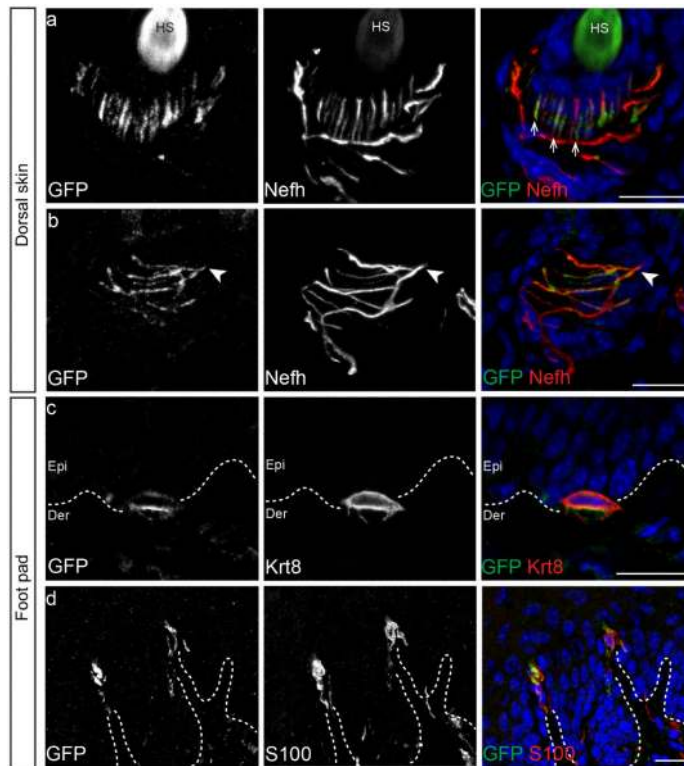


Figure 1. Piezo2 is localized at the nerve terminals of sensory neurons that innervate the skin **a and b**, representative images of immunostaining of GFP, Nefn and DAPI (blue) in the hair follicle of the *Piezo2-GFP* dorsal skin. GFP staining indicates localization of the Piezo2-GFP fusion protein and Nefn marks myelinated neurons. **c**, representative image of immunostaining of GFP, Krt8, a specific marker of Merkel cells, and DAPI (blue) in the *Piezo2-GFP* glabrous skin. **d**, representative images of immunostaining of GFP and S100, a marker of Schwann cells, in glabrous skin. Arrows mark lanceolate endings (a) and arrowheads mark circumferential fibers (b). Dashed lines demarcate epidermal-dermal junction (c and d). HS, hair shaft; Epi, epidermis; Der, dermis. Scale bars (a-d) 20 μ m.

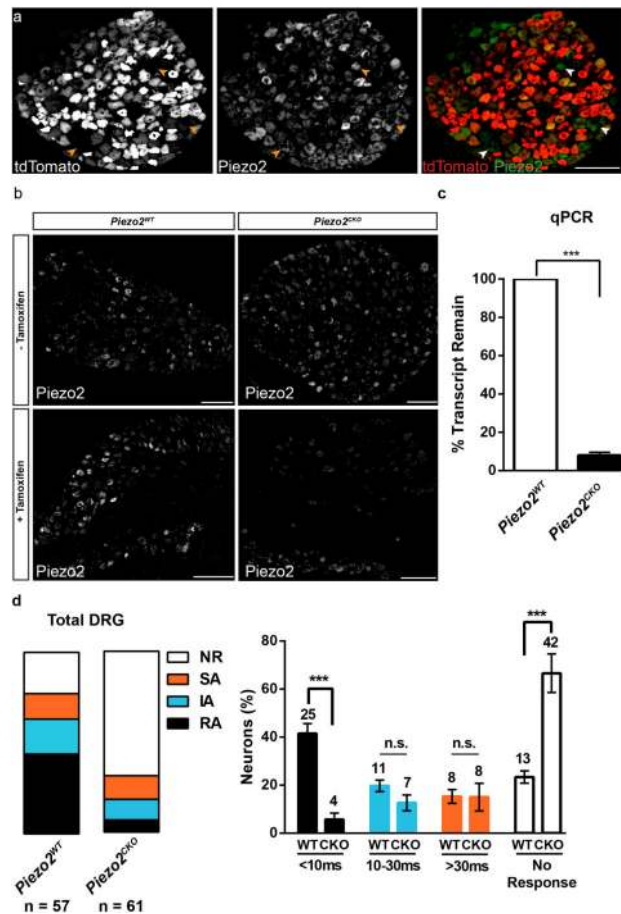


Figure 2. AvCreERT2 mediates efficient deletion of Piezo2 and leads to specific loss of rapidly adapting (RA) mechanically activated (MA) currents in cultured DRG neurons

a, Immunostaining of DRG neurons from tamoxifen-treated *AvCreERT2* x *Ai9* mice for tdTomato epifluorescence and Piezo2 antibody. Arrowheads indicate the relatively few tdTomato⁻/Piezo2⁺ neurons that would presumably not be deleted in *Piezo2^{CKO}* mice. **b**, Representative images of immunostaining using Piezo2 antibody in DRGs from *AvCreERT2* x *Piezo2^{loxP}* mice before and after tamoxifen treatment. **c**, qPCR of *Piezo2* from isolated DRGs from *Piezo2^{WT}* and *Piezo2^{CKO}* mice with *Piezo2^{WT}* values normalized at 100% (n = 3 independent experiments, P < .0001, Student's *t*-test). **d**, The proportion of DRG neurons responding with rapidly (RA, τ_{inact} <10ms), intermediate (IA, τ_{inact} 10-30ms), and slowly (SA, τ_{inact} >30ms) adapting MA currents from *Piezo2^{WT}* and *Piezo2^{CKO}* littermates. NR, non-responsive to displacements of at least one-third cell diameter. Results from n = 3 independent experiments. Error bars represent SEM, *** P < 0.001 for RA and *** P < 0.005 for NR, Student's *t*-test. Scale bars (a, b) 100 μ m.

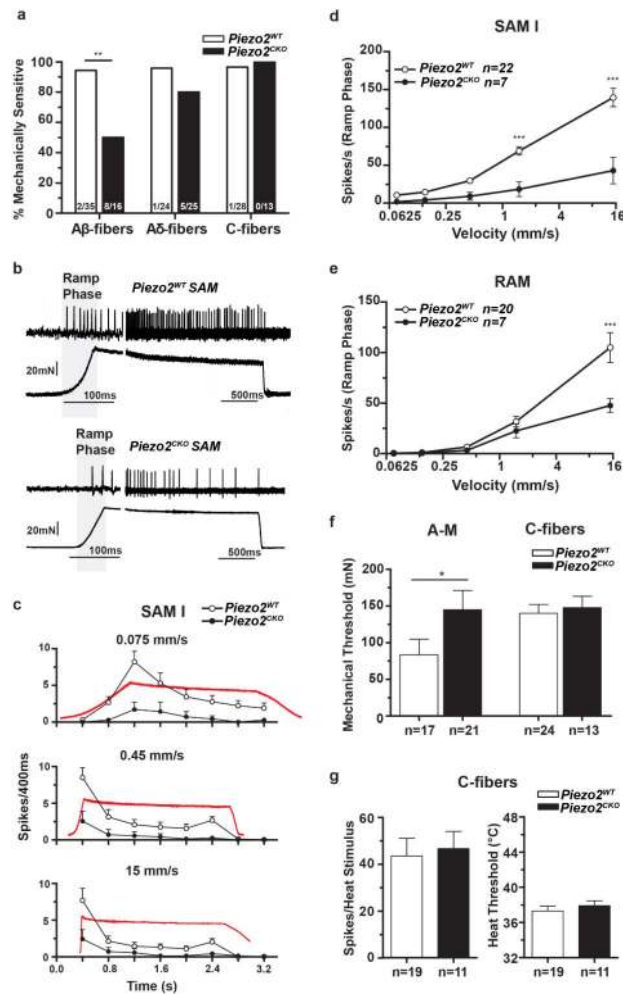


Figure 3. Piezo2 is required for mechanoreceptor function in *ex vivo* skin nerve preparation

a, Proportions of mechanically sensitive Aβ- and Aδ- and C-fibers in *Piezo2*^{CKO} mice compared to *Piezo2*^{WT} controls, Fisher's exact test ** P<0.01, one sided. **b**, Typical examples of SAM I mechanoreceptor responses from *Piezo2*^{CKO} and *Piezo2*^{WT} mice. **c**, Mean discharge rates (400 ms bins) during the course of ramp and hold stimuli with different onset velocities for SAM I receptors. Note the almost complete lack of dynamic ramp discharge in SAM I's recorded from *Piezo2*^{CKO} mice. **d**, Normally, SAM I discharge rates increase with increasing ramp speed, however SAM I receptors from *Piezo2*^{CKO} mice showed a strong reduction in velocity sensitivity with firing discharge increasing only marginally with increasing stimulus velocity, (repeated measures ANOVA, F=19.69, P<0.0001, with Bonferroni post-hoc test, ***P<0.001). **e**, Rapidly adapting afferents also displayed reduced velocity sensitivity in *Piezo2*^{CKO} mutant mice (repeated measures ANOVA, F=4.36, P<0.05, with Bonferroni posthoc test, ***P<0.001). **f**, Mean force thresholds for nociceptor discharge. Individual nociceptors threshold were calculated by averaging the thresholds of first spikes occurring during the stimulus ramp phase for all 6 stimuli applied. (A-Ms, left; C-fibers right). Note significant elevation of mechanical thresholds for A-Ms in *Piezo2*^{CKO} mice (Mann-Whitney test, * P<0.05), but no change in C-fibers mechanical thresholds. **g**, Discharge rates and heat thresholds to standard noxious heat

ramps did not differ between polymodal C-fibers recorded from *Piezo2^{CKO}* and *Piezo2^{WT}* mice. Data are presented as mean \pm SEM.

Author Manuscript

Author Manuscript

Author Manuscript

Author Manuscript

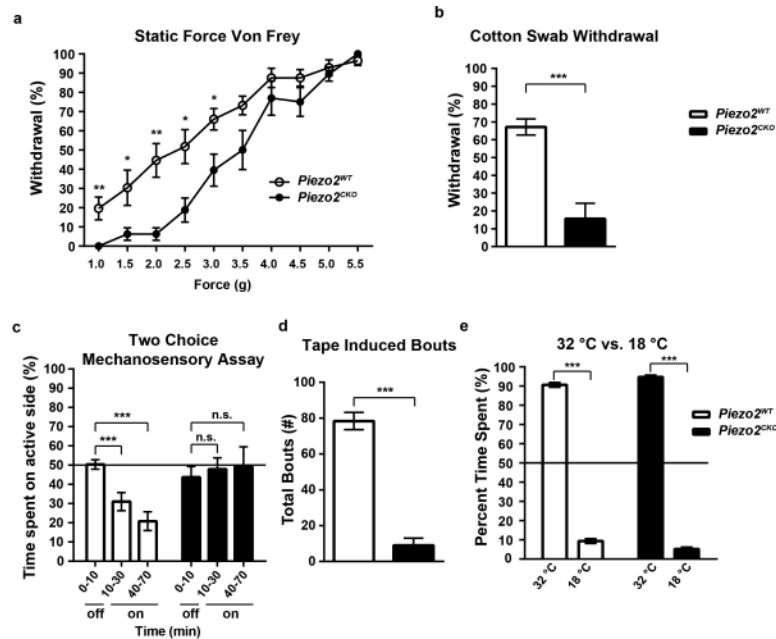


Figure 4. Piezo2^{CKO} mice show profound and specific defects in innocuous touch sensation in multiple behavioral assays

a, Percent response to varying forces of von Frey filaments in *Piezo2^{WT}* (n = 14) and *Piezo2^{CKO}* mice (n = 12). **b**, Percent response to a sweep of cotton on the hind paw in *Piezo2^{WT}* (n = 14) and *Piezo2^{CKO}* mice (n = 9). Of note, 6 out of 9 *Piezo2^{CKO}* mice showed zero responses to the cotton stimulus. **c**, Time spent on the mechanically active side over the course of 1 hour, with 10 minutes of no stimulation on either side (“off”), *Piezo2^{WT}* (n = 15) and *Piezo2^{CKO}* mice (n = 11). **d**, Number of bouts in response to a 3 cm piece of adhesive tape affixed to the back of a mouse over a 5 minute period in *Piezo2^{WT}* (n = 14) and *Piezo2^{CKO}* mice (n = 10). **e**, Percent time spent on either side of a two choice assay with one zone set at 18 °C and one zone set at 32 °C in *Piezo2^{WT}* (n = 13) and *Piezo2^{CKO}* mice (n = 10). Error bars represent SEM, all experiments performed with at least n = 4 separate cohorts of both male and female littermate control mice, * P < 0.05, ** P < 0.005, *** P < 0.0005, Mann Whitney non-parametric analysis.